Photo-responsive supramolecular polymer bottle-brushes: The key role of the solvent on self-assembly and responsiveness

Luke Harvey, Ralf Schweins, Isabelle Morfin, Gilbert Chahine, Guillaume Brotons, Laurent Bouteiller, Erwan Nicol, Olivier Colombani

Photo-responsive supramolecular polymer bottle-brushes: the key role of the solvent on self-assembly and responsiveness

Luke Harvey[a], *Ralf Schweins*[b], *Isabelle Morfin*[c], *Gilbert Chahine*[d], *Guillaume Brotons*[a], *Laurent Bouteiller*[e], *Erwan Nicol*[a*], *Olivier Colombani*[a*]

[a] Institut des Molécules et Matériaux du Mans (IMMM), UMR 6283 CNRS, Le Mans Université, 72085 Le Mans, Cedex 9, France. luke.harvey.etu@univ-lemans.fr; guillaume.brotons@univ-lemans.fr; Erwan.nicol@univ-lemans.fr (corresponding author); olivier.colombani@univ-lemans.fr (corresponding author)

[b] Institut Max von Laue - Paul Langevin, DS / LSS, 71 Av. des Martyrs, F-38042 Grenoble, France. schweins@ill.eu

[c] Université Grenoble Alpes, LiPhy, F-38000, Grenoble, France. isabelle.morfin@univ-grenoble-alpes.fr

[d] SIMaP, Grenoble INP, CNRS, Université Grenoble Alpes, 38000 Grenoble, France. gilbert.chahine@esrf.fr

[e] Sorbonne Université, CNRS, Institut Parisien de Chimie Moléculaire, Equipe Chimie des Polymères, 4 Place Jussieu, F-75005 Paris, France. laurent.bouteiller@upmc.fr

ABSTRACT

Hypothesis. Supramolecular polymer bottlebrushes (SPBs) consist in the 1D self-assembly of building blocks composed of a self-assembling core with pendant polymer arms. Kinetic hurdles often hinder their stimuli-responsiveness in solution. Changing the nature of the solvent should alleviate these hurdles by modulating the self-association strength, leading to stimuli-responsive SPBs.

Experiments. The SPBs were formed, in various solvents, by hydrogen bond-driven self-assembly of an azobenzene-bisurea decorated with poly(ethylene oxide) polymer arms. The photo-isomerization of the azobenzene unit was studied by UV/visible spectroscopy and proton NMR spectroscopy, whereas the consequences on supramolecular self-assembly were studied by small angle neutron and X-ray scattering.

Findings. In water, the assembly was previously shown to be driven by both hydrogen-bonds and strong hydrophobic effects, the latter rendering the system kinetically frozen and the disassembly irreversible. Here we show that in organic solvents such as toluene or chloroform, reversible light-responsive dissociation is achieved. Solvophobic effects in these solvents are expected to be much weaker than in water, which probably allows reversibility of the light-response in the former solvents. The key role of the solvent on the reversibility of the process opens up new perspectives for the design of stimuli-responsive SPBs and their applications in various fields.

Key words: nanocylinders, supramolecular chemistry, self-assembly, bottle-brush polymers, photo-responsiveness, solvant effects, reversibility

Introduction

Supramolecular polymer bottlebrushes (SPBs) consist in the 1D self-assembly of macromolecular building blocks composed of a self-assembling core with pendant polymer arms. Their formation is generally achieved in solution through cooperative and directional non covalent interactions, such as π-stacking or hydrogen-bonding, often complemented by the hydrophobic effect (in aqueous environment).[1,2] Compared to supramolecular 1D-nanostructures formed by small organic molecules[3], SPBs allow for introducing more diverse functionalities due to the large variety of polymers available, which is relevant for a wider panel of applications. For instance, using polymeric arms permits the synthesis of artificial light-harvesting supramolecular nanotubes by aligning chromophores along the 1D-assemblies allowing efficient Förster resonance energy transfer while avoiding aggregation-induced quenching of the chromophores[4]. The incompatibility between two polymer arms, grafted on each side of the core, was also used to promote segregation of the arms on either side of cyclic peptide-polymer nanotubes, creating Janus SPBs able to form artificial pores when inserted in phospholipid membranes.[5] Other Janus SPBs were reported to efficiently stabilize oil-in-water emulsions.[6]

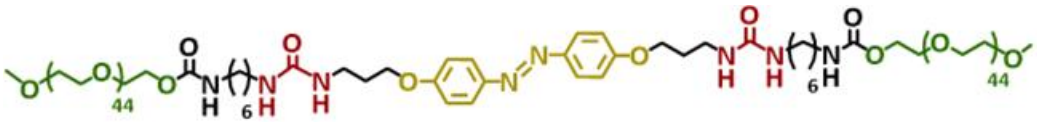

Scheme 1. Chemical structure of Azo-(U-PEO)$_2$.

Due to the non-covalent nature of their backbone, SPBs are attractive candidates for the elaboration of stimuli-sensitive assemblies, whereby stimuli triggered disassembly can be achieved. While several examples of stimuli-sensitive SPBs have been reported[7–10], most rely on the polymer arms to impart responsiveness, which limits the versatility of the approach. Relying on the self-assembling core is therefore a more versatile approach. However, only a

handful of studies achieved this, using stimuli such as pH[9], oxidation[7,10] , host-guest chemistry[8], or light[11]. Light is a particularly attractive stimulus since it can be easily fine-tuned in terms of wavelength and intensity, allows a high spatio-temporal control, and is non-invasive. Light-responsive 1D-supramolecular self-assemblies based on small molecules have already been reported.[12–18] However, SPBs are more complicated to obtain than supramolecular 1D-nanostructures formed by small organic molecules due to steric hindrance of the polymer arms and the loss of conformational entropy which tend to hinder self-assembly.[19,20]

To the best of our knowledge, there are only two reported examples of light-triggered disassembly of SPBs in the literature, one of them relying again on the nature of the polymer arms to impart responsiveness.[21] In the other work, our group reported the synthesis, self-assembly in aqueous medium and light-triggered disassembly of a poly(ethylene oxide) (PEO)-based supramolecular precursor (Azo-(U-PEO)$_2$) (**Scheme 1**).[11] This compound combines a photo-responsive azobenzene unit, hydrogen bonding ureas, C_6 alkyl spacers to reinforce the hydrogen bonding units in water through the solvophobic effect and PEO arms granting solubility both in aqueous medium and organic solvents. In aqueous solution and in the *trans* configuration of the azobenzene core, this polymer was shown to form thin (radius = 5 nm) SPBs several hundreds of nanometers long. UV irradiation photo-isomerized a large portion of the azobenzene to *cis* configuration (~75%), triggering the disassembly of the nanocylinders into small spherical structures. Blue-light irradiation switched back the azobenzene to their *trans* configuration, but did not induce the re-assembly into nanocylinders because the assemblies were kinetically frozen (formed out of thermodynamic equilibrium).

In the present study, we aimed at obtaining reversibly light-responsive supramolecular SPBs, which requires that the self-assemblies are formed under thermodynamic equilibrium. Based on the literature on polymer self-assembly in solution[16,17,22,23], we speculated that

reducing solvophobic effects by switching from water to organic solvent would help forming SPB under thermodynamic equilibrium able to reversibly photo-switch. We therefore investigated the supramolecular 1D-self-assembly of Azo-(U-PEO)$_2$ in toluene and chloroform, organic solvents with different hydrogen bond competing abilities and displaying weaker solvophobic effects,[16] with the objective to obtain reversibly-light-responsive SPBs for the first time.

Materials and methods

Materials

The synthesis and chemical characterization of Azo-(U-PEO)$_2$ (**Scheme 1**) was reported elsewhere.[11] Deuterated solvents (toluene-d_8, $CDCl_3$, DMSO-d_6 and D_2O) and standard solvents were purchased from Aldrich.

Methods

Nuclear magnetic resonance (NMR). ^{1}H NMR spectra were recorded on either a Bruker DPX-200 or Bruker AC-400 spectrometer, using deuterated chloroform ($CDCl_3$) or dimethyl sulfoxide (DMSO-d_6), and toluene-d_8/DMSO-d_6 mixtures as solvents. Chemical shifts (δ) are expressed in parts per million (ppm) relative to the reference (tetramethylsilane (TMS), δ = 0 ppm). Multiplicities are reported as follows: singlet (s), doublet (d), triplet (t), quadruplet (q), quintet (qt), sextet (sext), multiplet (m), and broad signal (br s).

Light irradiations. LED irradiations were carried out using a Thor Labs DC2200 High-Power LED Driver, with Thor Labs M365LP1 and Thor Labs M450LP1 LEDs, operating at 365 nm and 450 nm, respectively. The LEDs were linked to the driver using a waveguide. Irradiation of SANS solutions was achieved for 15 min by first irradiating the solution in a vial under gentle stirring at full power, with the waveguide placed 4.5 cm above the solution. The LED irradiance at this distance was measured using a Thor Labs PM160T optical power

meter, and the irradiances were measured as follows: 215 $mW.cm^{-2}$ for the 365 nm LED and 515 $mW.cm^{-2}$ for the 450 nm LED. The irradiated SANS solutions were then transferred to Banjo cells for SANS analysis. Irradiation of solutions for UV-Vis analysis were carried out in the same manner, with varying irradiation times. Irradiations during SAXS analysis were achieved directly on the beamline by placing the LED setup on the beamline, with the LED waveguide at approximately 5 cm from the quartz capillary. The irradiation times corresponds to those indicated on the corresponding figures (Figures 6 and S14).

UV-Vis absorption spectroscopy. UV-Vis spectra were measured on a Jasco V760 spectrometer using glass cuvettes with an optical pathway of 1 mm at room temperature.

Small angle neutron scattering (SANS). SANS measurements were performed in 2 mm Banjo Cells at the Institut Laue-Langevin (ILL, Grenoble, France), on the small angle neutron scattering instrument D22. A circular neutron beam was used (diameter of 13 mm). The D22 instrument uses two detectors: a front detector, at a fixed distance of 1.4 m (relative to the sample), as well as a rear detector. Measurements were achieved using a sample to rear detector distances at 17.6 m (collimation), using a neutron wavelength of 6 Å. This setup allowed for probing over a wide q-range: 0.0026 $Å^{-1}$ to 0.6424 $Å^{-1}$. Neutron detection was achieved using two ^{3}He detectors (multi-tube detector consisting of vertically aligned Reuter-Stokes tubes, with 128 tubes for the rear and 96 tubes for the front detector, all with a diameter of 8 mm and a pixel size of 8 mm x 8 mm). Acquired detector images were reduced using GRASP software, to correct for the transmission of the direct beam, to scale to absolute intensity, and to azimuthally average. Scattering contribution of the empty cell and solvent were subtracted from the scattering curves.

SANS fitting. The SANS data were fitted using SASView application (*http://www.sasview.org/)*.

Small angle X-ray scattering (SAXS). X-ray scattering experiments were performed in 1.5 mm quartz capillaries using the WAXS-SAXS setup at the D2AM beamline of the European Synchrotron Radiation Facility (ESRF, Grenoble, France). The samples were probed with a monochromatic X-ray of 12 keV ($\lambda = 1$ Å). The scattering intensity was measured using a two-dimensional SAXS pixel detector (XPAD-WOS). The sample-detector distance was 3.29 m allowing to cover scattering vector ranges of $q = 3.10^{-3}$ to $2.4.10^{-1}$ $Å^{-1}$. q-range and radial averaging were determined measuring Ag and LaB_6 standards. Glassy carbon was used as reference to obtain the scattered intensity in absolute unit. Jupyter notebook script was used to perform the radial averaging, correct for the transmission, and obtain the I(q) data.

Results and discussion

Self-assembly of trans-Azo-(U-PEO)$_2$ in chloroform and toluene.

Assemblies in toluene and chloroform were probed using small angle X-ray (SAXS) and neutron (SANS) scattering experiments. Solutions were prepared by directly dissolving the polymer in deuterated solvent at C=10 g/L. This concentration was selected based on previous SANS studies conducted on other 1D self-assembling polymers which showed that a proper signal-to-noise ratio is obtained between 1 and 10 g/L for well contrasted polymers.[6,20,25] It was moreover verified in toluene that the scattering profile normalized by concentration does not significantly change at 5 or 10 g/L (see **Figure S1-top**). This implies that inter-particle interactions are negligible in this concentration range and that the assemblies do not depend on concentration in this range, making the selected concentration relevant. SANS analysis of solutions in toluene-d_8 or $CDCl_3$ showed a q^{-1} angular dependency at low q values (**Figure 1**), which is expected for anisotropic 1D nanocylinders. The total length L of the nanocylinders exceeded the q-range accessible by SANS (the Guinier plateau was not reached even at $q_{min} = 3\times10^{-3}$ $Å^{-1}$) so that its value could not be determined. Based on the q-range on which a q^{-1}

dependency was observed, L was nevertheless estimated to be at least higher than 100 nm, see section 1 of the SI for details. Overall, these results indicate that supramolecular nanocylinders formed spontaneously in organic solvents, whereas a co-solvent approach was required in aqueous solution[11] and therefore suggests that the assemblies form under thermodynamic equilibrium.

In toluene, the scattered intensity was high, allowing to characterize the solution over a large q-range (**Figure 1**). The data revealed the contribution from very small objects at high q-values ($q > 0.1$ Å^{-1}), which may correspond to the presence of very small particles in solution (free or weakly associated polymer chains) and/or to the large-q contribution of hairy cylinders as in the model proposed by Pedersen et al.[24] To simplify fitting, the data above $q = 0.1$ Å^{-1} were fit using a Gaussian coil model, which gave an $R_g = 1.5$ nm (see **Figure S1** for details). This contribution was then subtracted from the experimental data, and the resulting scattering curve was fit using different cylinder models. In this way we neglect the interference terms related to the correlation of the positions between the large scale cylinders responsible for the high intensities at small angles and smaller scatterers (unassociated Gaussian chains or polymer hairs attached to the cylinders), responsible for the weak signal measured above $q = 0.1$ Å^{-1}. Fitting the data using a homogenous cylinder model with dispersity on the radius gave poor results and did not fit the data well (see **Figure S2**). A core-shell cylinder model with a higher contrast for the core than for the shell gave better fits (see **Figure S3**). This strongly suggests that the core is hardly solvated, whereas the shell consists of solvated polymer arms (the shell was estimated to be solvated by about 50% of toluene-d_8 by volume, see section 2 of the SI for details); a reasonable result for the self-assembled nanocylinders. Both the homogeneous cylinder and the core-shell cylinder models led to a consistent estimation of the total radius of the nanocylinders around 6 nm, which is close to the values estimated in water,[11] giving credit to the estimated value (see section 1 of the SI for

details). Finally, the contribution of the Gaussian coils at high q was added to the fit (see **Figure 1** and **Figure S3** for details), yielding a reasonable agreement between the experimental data and the fit. Note that the quality of the fit may have been further improved by using more complex models, although this was not attempted here (see section 1 in the SI). Finally, the molar mass per unit length within the section of the nanocylinders was estimated (see section 3 of the SI), indicating that the cross-section of the nanocylinders contain about 1.5 molecules. Given the approximations made to estimate this value, it can be considered reasonably close to 1, as expected for isolated nanocylinders with no significant lateral aggregation. This result is consistent with the fact that the solvophobic effect is supposed to be weak in toluene,[16] mostly suppressing lateral aggregation of the nanocylinders.

The intensity scattered by the solution in $CDCl_3$ was much lower than that in toluene-d_8; which can to a large extent be explained by a much lower contrast of the polymer in $CDCl_3$ than in toluene-d_8 (**Figure S4**). Additionally, fitting of the data in $CDCl_3$ (**Figure 1**) with a model of homogeneous nanocylinders (the scattered intensity was not sufficient at high q to distinguish between different cylinder models as in toluene-d_8 and the simplest model was therefore used here) suggests that the amount of solvent swelling the assemblies was higher in $CDCl_3$ (~ 85%) than in toluene-d_8 (~ 50%). This further decreases the effective contrast in the former solvent. The mass per unit length of the nanocylinders estimated in $CDCl_3$ corresponded to 0.6 molecules in the cross-section, again in reasonable agreement with the expected value of 1 in the absence of lateral aggregation (see SI section 4 for details).

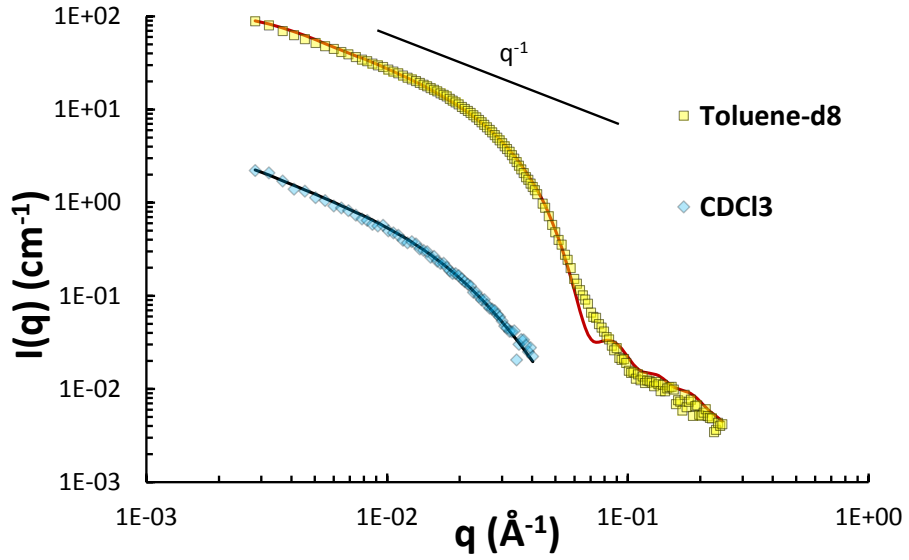

Figure 1. SANS data (in cm^{-1}) of Azo-$(U\text{-}PEO)_2$ in toluene-d_8 and $CDCl_3$ at 10 g/L (points) and their respective fits (solid lines). Due to the low scattering intensity of the chloroform solution, data beyond q = 0.03 $Å^{-1}$ were unreliable. The data for the $CDCl_3$ solution were fit using a homogeneous cylinder model with L > 100 nm, r = 3.4 nm (lognormal distribution, PD = 0.496) and SLD = $2.74.10^{-6}$ $Å^{-2}$ (solvent SLD = $3.16.10^{-6}$ $Å^{-2}$, scale = 8.4 vol%). The data for the toluene solution were fit using a combination of a core-shell cylinder model, with L > 100 nm, r_{core} = 3.2 nm (lognormal distribution, PD = 0.124, SLD_{core} = $1.34.10^{-6}$ $Å^{-2}$) and r_{shell} = 2.9 nm (lognormal distribution, PD = 0.064, SLD_{shell} = $3.0.10^{-6}$ $Å^{-2}$) (solvent SLD = $5.66.10^{-6}$ $Å^{-2}$, scale = 8.4 vol%), corresponding to an overall radius of 6.1 nm and a Gaussian coil model (R_g = 1.5 nm, i_zero = 0.029 cm^{-1}). Details are given in **Figures S1-3**.

After having confirmed that Azo-$(U\text{-}PEO)_2$ self-assembles in $CDCl_3$ and toluene-d_8 into nanocylinders, its light-responsiveness was studied, first by probing the ability of the azobenzene unit to undergo photo-isomerization, and then by evaluating the impact of the photo-isomerization on the self-assembly.

Probing the *trans* → *cis* and *cis* → *trans* photo-isomerizations by UV-vis and ^{1}H NMR.

Photo-isomerization kinetics were measured by UV-Vis spectroscopy (**Figures 2 and 3**) and *trans*/*cis* isomer ratios at the photo-stationary states were assessed by ^{1}H NMR experiments (**See Figures S5-S9**).

In chloroform

In chloroform, ^{1}H NMR indicated that 100% *trans*-Azo was present in the initial solution (see **Figure S5**). The initial UV-Vis spectrum (**Figure 2)** showed a maximum of absorption in the UV domain at 360 nm, which corresponds to the $\pi \rightarrow \pi^*$ transition of *trans*-Azo. Irradiating this solution with UV light (365 nm) triggered photo-isomerization to *cis*-Azo. This was evidenced in UV-Vis (**Figure 2**) by the progressive diminution of the intensity at 360 nm to ~10% of its initial value and to a change of this peak's shape. Concomitantly two new maxima appear, respectively at 320 and 450 nm, the former corresponding to the $\pi \rightarrow \pi^*$ transition and the latter to the $n \rightarrow \pi^*$ transition of *cis*-Azo. The kinetic plots of the photo-isomerizations are presented in **Figure S6**, and the kinetics in chloroform appeared to be similar to those in water.[11] ^{1}H NMR (**Figure S5**) indicated a *trans*/*cis* ratio of 10/90, consistent with UV-Vis (see **Figure 2**).

The chloroform solution was then irradiated a second time with blue light (450 nm) in order to trigger *cis* → *trans* photo-isomerization. The absorption band at 450 nm rapidly (photo-stationary state reached within less than 1 min) decreased while the UV maxima of the *trans*-Azo re-appeared (see **Figure 2**). Note that only 70% of the initial intensity at 360 nm was recovered, suggesting that not all of the azobenzenes were converted back to their *trans* configuration. This result was consistent with ^{1}H NMR which indicated a *trans*/*cis* ratio of ~75/25 at steady-state after irradiation at 450 nm (**Figure S5**). This behavior was already observed in aqueous medium[11] and attributed to the fact that irradiation at 450 nm not only triggers the *cis*-*trans* isomerization, but also the *trans*-*cis* one, albeit with different quantum

yields. The *trans*/*cis* photo-stationary state therefore depends on the respective quantum yields of both photo-isomerization mechanisms at 450 nm and does not correspond to 100% *trans*. Slightly heating the solution in the dark nevertheless allowed for 100% conversion to *trans*-Azo (see **Figure 2**), proving the reversibility of the transition. UV (365 nm)/blue light (450 nm) irradiation cycles were performed, and led to identical photo-stationary states, indicating that no degradation occurred during photo-isomerizations (see **Figure S7**). Lastly, thermal relaxation kinetics of *cis*-Azo back to *trans*-Azo were monitored using UV-Vis, indicating a half-life of 12 hours at room temperature (20°C) (see **Figure S8**). This relatively slow thermal relaxation allowed for reliable characterization of assemblies within the measurement timeframe.

In toluene

The same experiments were repeated in toluene. However, in these conditions direct analysis of the toluene-d_8 solution by ^{1}H NMR was not possible because of a lack of resolution of the ^{1}H NMR spectrum in this solvent. This could be attributed to the poor solvation of the azobenzene self-assembling core (4,4'-dihydroxyazobenzene was indeed fully soluble in chloroform at 0.05 g/L, corresponding to the same molar concentration as for Azo-(U-PEO)$_2$ at 1 g/L, but only partially soluble in toluene) and/or to a strong self-assembly in toluene with slower exchange dynamics in this solvent than in $CDCl_3$. The resolution of the ^{1}H NMR spectra in aqueous medium was also poor, for the same potential reasons.[11] This technical issue was circumvented by irradiating in pure toluene-d_8 (to avoid any contribution of DMSO-d_6) and, then, adding 10 vol.% DMSO-d_6 to the solution prior to analysis, see **Figure S9** for details. ^{1}H NMR confirmed that 100% *trans*-Azo was also initially present in toluene-d_8 (see **Figure S9**). The initial solution showed a significant hypsochromic effect: the UV absorption maximum was shifted from 360 nm in chloroform to 325 nm in toluene (see

Figures 2 and 3). Note that the maximum was also ~360 nm in water[11] or DMSO (See **Figure S10**). In order to determine if this effect was due to the solvent, 4,4'-dihydroxyazobenzene was selected as a molecular model of azobenzene. UV-Vis analysis indicated that the maxima were close for this model compound in toluene, $CHCl_3$ and water (~ 355 +/- 5 nm nm) and slightly red-shifted in DMSO (~ 370 nm, see **Figure S11**). This means that the hypsochromic shift observed with Azo-(U-PEO)$_2$ in toluene is not due to solvatochromism but to another effect. It is possible that the assembly in toluene induces a different packing compared to the assembly in other solvents, thereby affecting its absorption spectrum.

Exposing this solution to UV irradiation (365 nm) again triggered *trans* → *cis* photo-isomerization, with the appearance of a band at 450 nm. The maximum at 325 nm simultaneously decreased, but with a much weaker deformation of the peak in toluene than in chloroform: the new maximum appearing upon *trans* → *cis* isomerization in toluene was observed at 320 nm, as in chloroform, implying a shift of 5 nm only. Because of the proximity of the maxima of the *trans* (325 nm) and the *cis* (320 nm) isomers in toluene, the *trans*/*cis* ratio after UV-irradiation at 365 nm was estimated using the value of the absorbance at 360 nm, where the contribution of the *cis*-isomer should be weaker. We stress that this methodology only gives a rough estimate of the *trans*/*cis* ratio which was ~ 25/75. These results were confirmed with ^{1}H NMR experiments in toluene-d$_8$/DMSO-d$_6$ 90/10 (v/v) mixtures, giving a 30/70 ratio (see **Figure S9**). We note that the *trans*/*cis* ratio at the photo-stationary state after irradiation at 365 nm is higher than in chloroform (**Figure S5**) or DMSO (see **Figure S12**) and of the same order of magnitude as in water.[11] Furthermore, *trans* → *cis* photo-isomerization kinetics in toluene were slower than in chloroform (**Figure S6**). Both effects might be due to a stronger self-assembly in water (due to hydrophobic effects) or in toluene (due to strong hydrogen bonding in this weak hydrogen bond competitor) compared to

chloroform (moderate H bond competitor) or DMSO (strong H bond competitor), slightly hindering photo-isomerization in the two former solvents. The hindrance is not strong though, as photo-isomerization still occurs to a large extent and remains quite fast in toluene or water. The slower and lower yielding isomerization in toluene may also be attributed to the hypsochromic effect discussed above, as the UV absorption maxima was further away from the irradiation wavelength.

Further irradiation at 450 nm in toluene led to recovery of the *trans* isomer. Moreover, in contrast to chloroform, ~100% of the initial intensity was recovered, indicating that the azobenzenes had almost quantitatively been isomerized back to their *trans* configuration (**Figure 3**). This observation could be related to the hypsochromic effect observed in toluene which might imply a change of the quantum yield of the *trans* → *cis* and *cis* → *trans* photo-isomerizations at 450 nm. Irradiation cycles were performed and photo-stationary states were again found to be reproducible (**Figure S13**). Lastly, thermal relaxation was also found to be rather slow, with a half-life of 10 hours (see **Figure S8**).

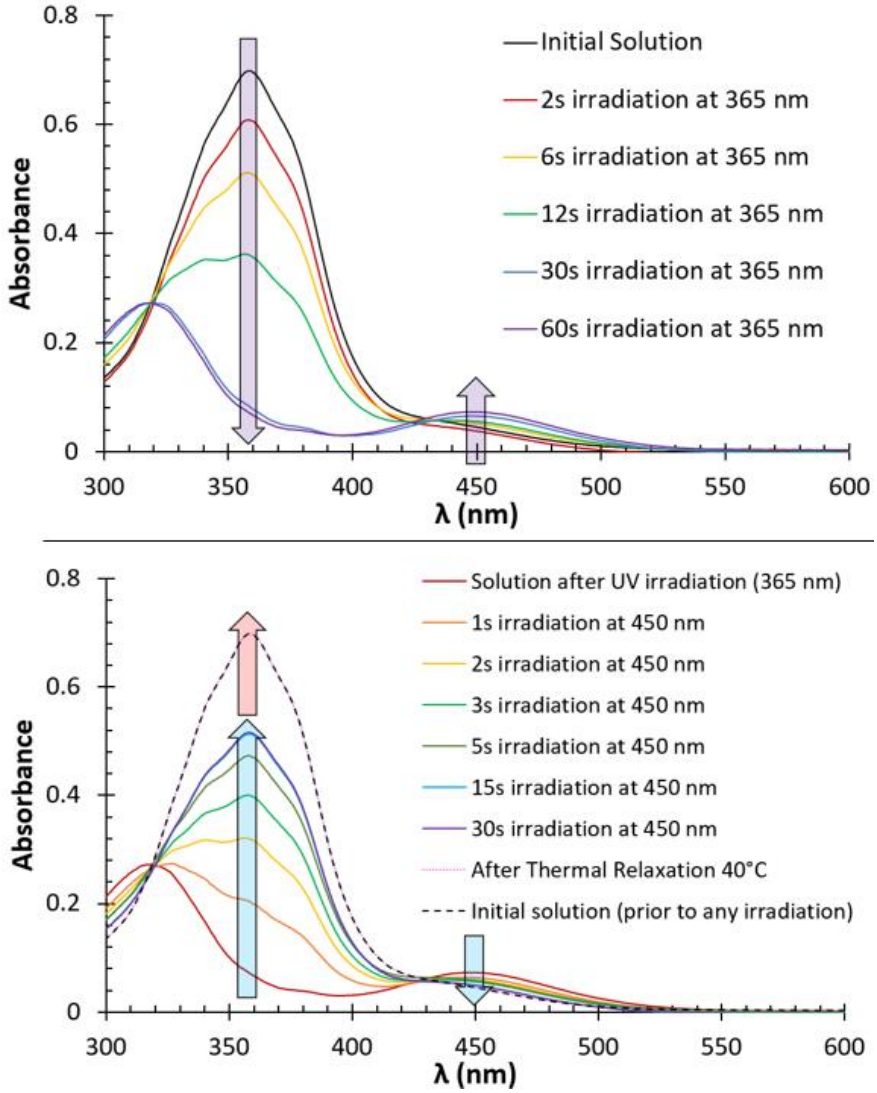

Figure 2. UV-Vis kinetics of photo-isomerization when irradiating with UV light (365 nm, top) and blue light (450 nm, bottom), followed by thermal relaxation at 40°C for 30 minutes (dotted line), at 1 g/L in $CHCl_3$. After blue light irradiation, the solution was heated at 40°C to promote thermal relaxation, and super-imposes with the UV spectra of the initial solution prior to any irradiation.

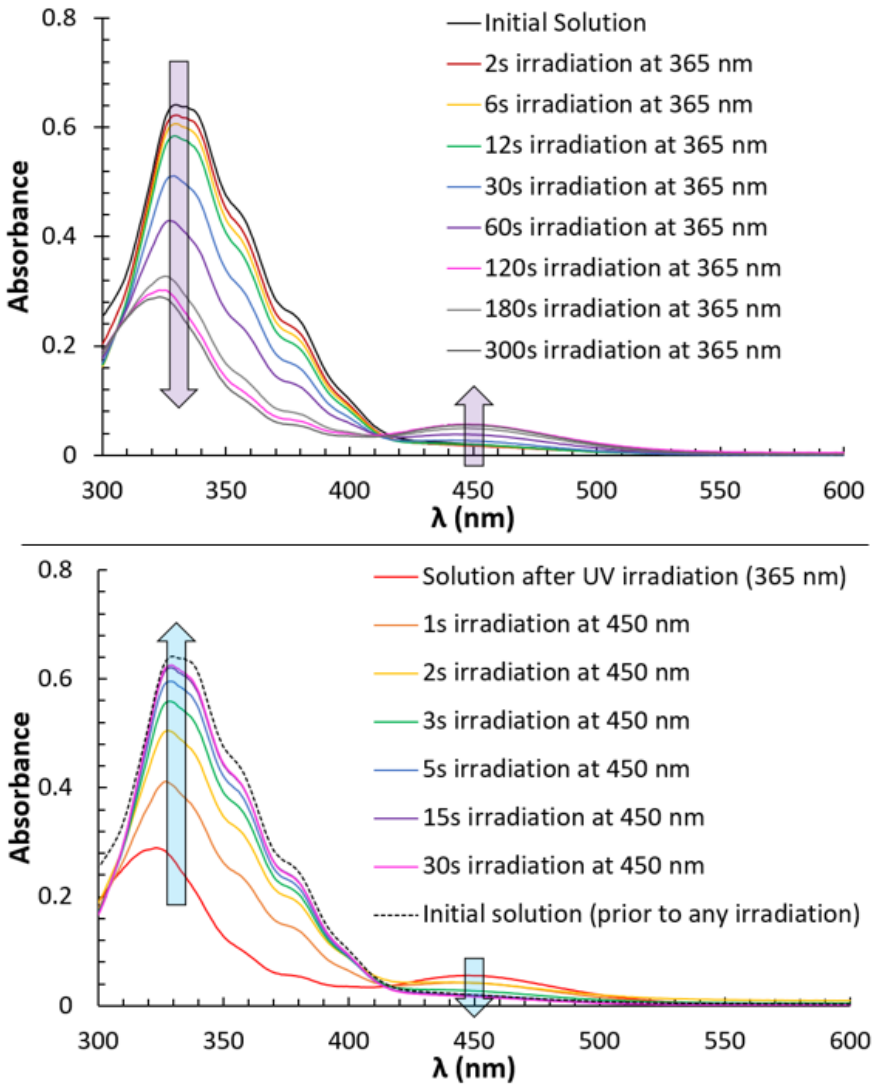

Figure 3. UV-Vis kinetics of photo-isomerization when irradiating with UV light (365 nm, top) and blue light (450 nm, bottom) at 1 g/L in toluene.

Impact of the photo-isomerization on self-assembly in $CDCl_3$.

After irradiation of the chloroform solution at 365 nm, SANS showed a drastic change of the scattering profile (**Figure 4**): the q^{-1} dependency was lost. The scattering intensity showed a q^{-3} dependence at low q-values, suggesting that some large aggregates were present. However, we stress that few very large particles would be sufficient to explain the q^{-3} dependency at low q as already observed for other systems.[25] After subtraction of the q^{-3}

contribution, the remaining signal exhibited no q-dependency at low q, suggesting that the solution mainly contains very small particles such as small Azo-(U-PEO)$_2$ aggregates. These data could indeed be fit using a Gaussian coil model, with a R_g = 4 nm. From the value of the scattered intensity at low q ($I_0 = 3.3.10^{-3}$ cm^{-1}), assuming that all polymer chains are involved in these small particles ($C = 10.10^{-3}$ $g.cm^{-3}$) and by estimating the contrast assuming that the polymer is not solvated ($K = 3.9.10^{-4}$ $mol.cm^2.g^{-2}$), the molar mass of these small particles was estimated to be $M_w = I_0/(KC) = 8.5.10^3$ g/mol, which is very close to $M_{unimer} = 4.9.10^3$ g/mol, confirming a very weak extent of aggregation.

Irradiating with blue light (450 nm) led to recovery of the nanocylinders with a q^{-1} dependence appearing again (**Figure 4**). Only 70% of the initial level of scattering was recovered though, consistent with the fact that only 70% of *trans*-azobenzene was recovered upon blue light irradiation.

As a conclusion, irradiation at 365 nm in $CDCl_3$ leads to almost quantitative *trans* → *cis* isomerization, accompanied by disruption of most cylinders. More importantly, both the photo-isomerization and the reassembly into nanocylinders is to a great extent reversible upon exposure at 450 nm.

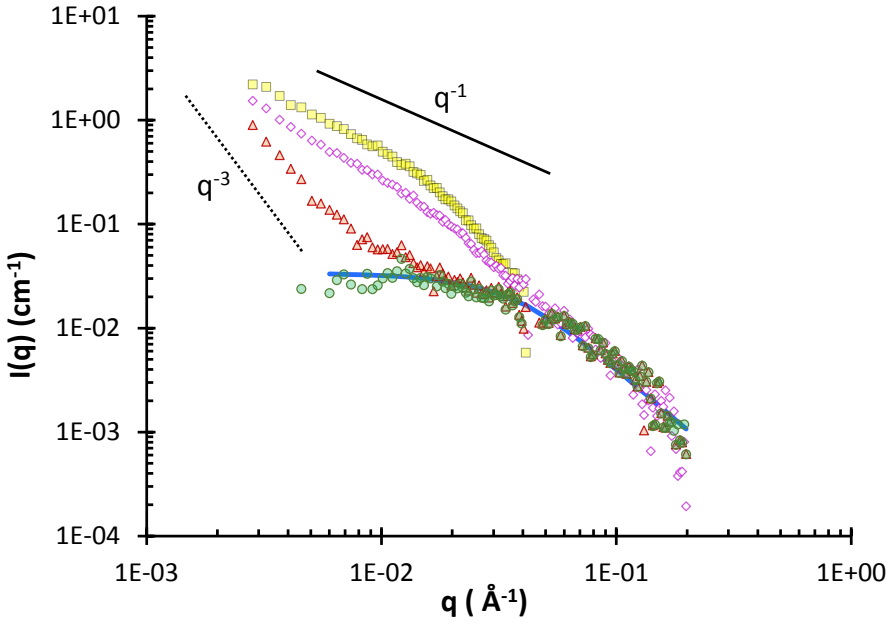

Figure 4. SANS data of a 10 g/L solution of Azo-(U-PEO)$_2$ in $CDCl_3$: (□) prior to irradiation, (△) after UV irradiation (365 nm), (○) same data after subtracting the q^{-3} dependence (these data were fitted with a Gaussian coil Sasview fit, R_g = 4 nm, —), and (◇) after a second irradiation with blue light (450 nm).

Impact of the photo-isomerization on self-assembly in toluene.

In toluene-d_8, exposure to UV irradiation (365 nm) led to a decrease of the SANS scattered intensity to approx. 30% of the initial intensity (**Figure 5**). However, the q^{-1} angular dependence was conserved indicating that nanocylinders were still present after irradiation. The scattering intensity at $q > 0.06$ Å^{-1} increased, suggesting a significant increase of the proportion of small particles, such as unimers or small aggregates formed from the disrupted nanocylinders. From the intensity scattered by these small particles and assuming that they are hardly aggregated (M_w close to that of unimers), their amount was estimated to correspond to ~ 80% of the weight concentration of polymers (see SI section 5 for details). Given the approximations made, this value agrees quite well with the fact that ~ 30% by weight of cylinders remain.

The q-range accessible by SANS does not allow determining whether the length of the cylinders was affected, but it is still at least > 100 nm after irradiation. Irradiating the sample with blue light (450 nm) led to the recovery of the initial scattered intensity, suggesting the disassembly is perfectly reversible (**Figure 5**).

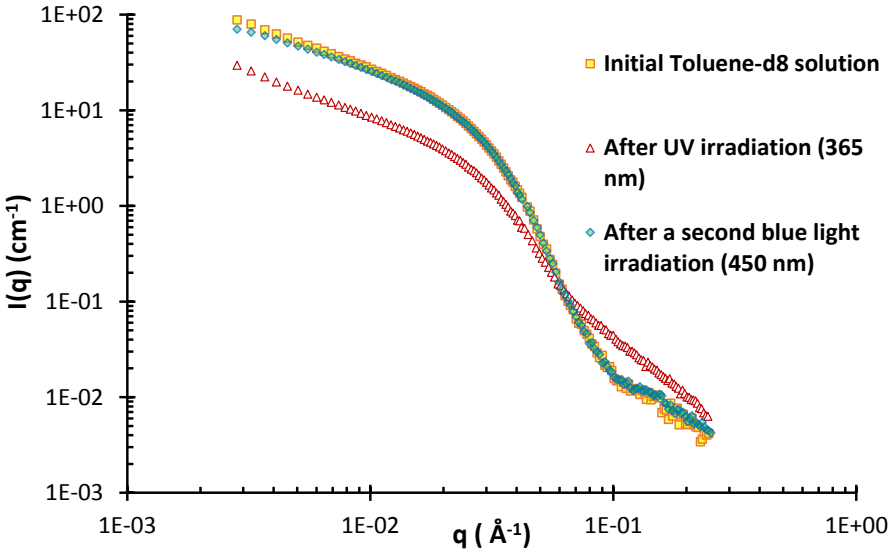

Figure 5. SANS data of (□) the initial toluene solution at 10 g/L, (△) after UV irradiation (365 nm), and (◇) after a second blue light irradiation (450 nm).

The photo-isomerization-induced disassembly and re-assembly was probed in more details by measuring kinetics of dissociation during exposure at 365 nm or 450 nm respectively. Given the rapidity of the photo-isomerization described above, very fast scattering measurements were necessary; which was achieved using synchrotron SAXS in toluene-d_8. Note that the same experiments could not be conducted in chloroform as this solvent absorbs too much for SAXS experiments. The initial SAXS scattering profile of the *trans*-Azo-(U-PEO)$_2$ solutions in toluene-d_8 is consistent with what was observed by SANS (**Figure S14**). As can be seen in **Figure 6 (top)**, the scattered intensity at 0.01 Å^{-1} rapidly diminished during exposure to 365 nm irradiation, until it reached ~ 20% of the initial intensity, which took ~ 180s. We note that after 180s, the scattered intensity (**Figure 6, top**) and the scattering curves (**Figure S14**) are nearly constant over time. This time is of the same order of magnitude as the time required to reach a steady *trans*/*cis* ratio under 365 nm irradiation (**Figure 3**). Additionally, the q^{-1} angular dependency is again maintained during irradiation at 365 nm,

suggesting that nanocylinders are still present when the *trans*/*cis* ratio becomes stable at the photo-stationary state (see **Figure S14**).

Upon blue light irradiation at λ=450 nm, the scattering intensity returned to its initial value within ~20 min (with a light intensity 10 times lower than that used for UV measurements) (**Figure 6, bottom**). Irradiation cycles were also performed and monitored by SAXS, and the assembly/disassembly was found to be reproducible, which confirmed the fact that no degradation occurred (**Figure S15**).

These results suggest that the nanocylinders are formed by *trans*-Azo-(U-PEO)$_2$ and that the rate-limiting step in the disassembly or reassembly process is the photo-isomerization. Indeed, the percentage of *trans* isomer at the photo-stationary state measured by UV-Vis and ^{1}H NMR spectroscopy after irradiation at 365 nm (25% or 30% respectively) is of the same order of magnitude as the amount of remaining cylinders determined by SANS or SAXS (30% or 20% respectively). Additionally, the time required to reach the photo-stationary state upon irradiation at 365 nm is of the same order of magnitude in UV-Vis (180 s to reach a constant amount of *trans*/*cis* isomers) and in SAXS (180 s to reach a constant scattering signal). The time required to reform the nanocylinders upon irradiation at 450 nm was longer (~ 20 min according to SAXS) than the time required to reach a photo-stationary *trans*/*cis* ratio (~ 30 s according to UV-Vis), but the SAXS experiments at 450 nm were conducted with a reduced intensity of the lamp (10% of the intensity used for the UV-Vis experiments). Finally, the SANS and SAXS experiments confirm full reversibility of the self-assembly in toluene upon exposure at 450 nm, coherent with UV-Vis measurements which showed that 100% of *trans* isomer was recovered upon exposure at this wavelength.

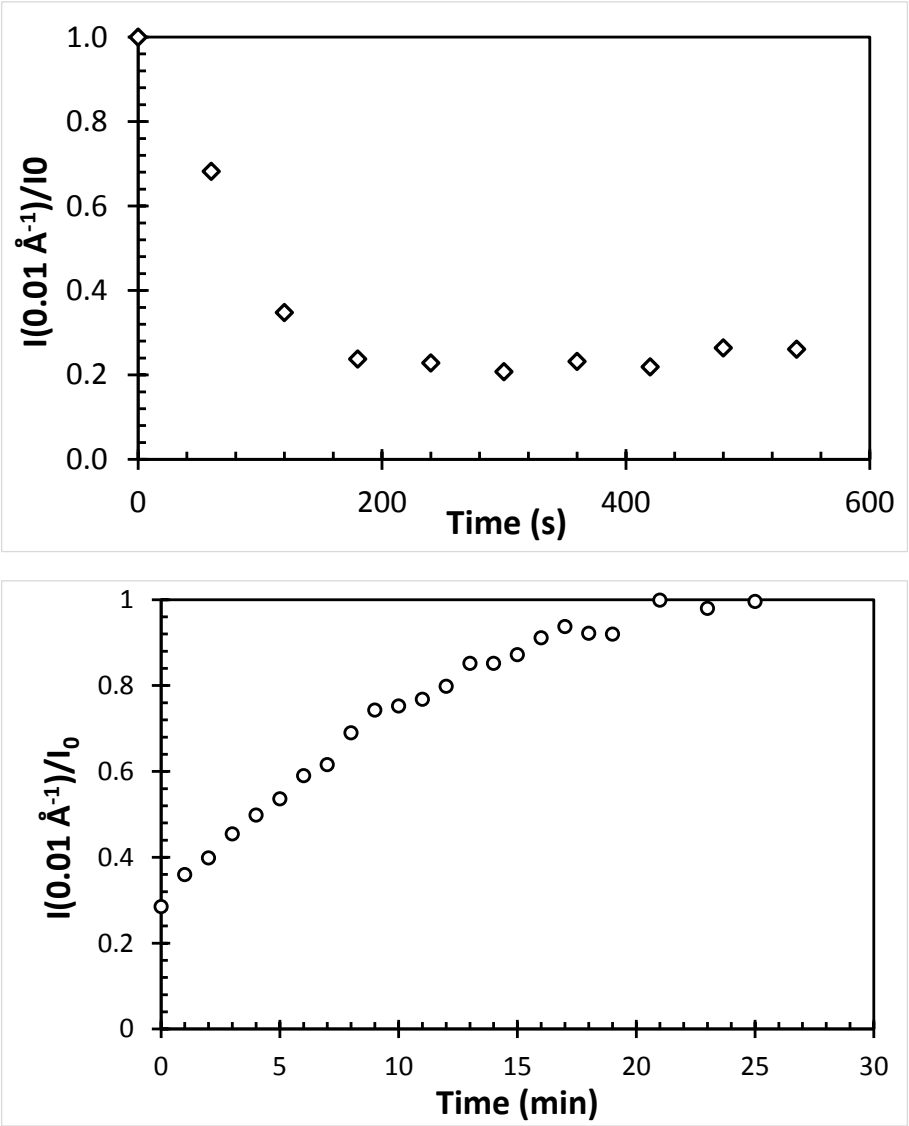

Figure 6. SAXS data of a 10 g/L solution of Azo-(U-PEO)$_2$ in toluene-d$_8$ during irradiation at 365 nm (**top**), during a second irradiation at 450 nm (at 10% of LED max. power) (**bottom**). The data plotted correspond to the scattering intensity at q = 0.01 Å^{-1} as a function of time normalized by its value before irradiation (i.e. I_{max} for the *trans*-isomer).

Summary: impact of the solvent on the extent of association and on the stimuli-responsiveness

Comparison of the results obtained in this work with those reported in our previous publication in aqueous medium suggests a strong impact of the solvent on the extent of self-assembly of Azo-(U-PEO)$_2$ and on its light responsiveness.

In our previous work,[11] it was observed that *trans*-Azo-(U-PEO)$_2$ formed out-of-equilibrium SPBs in aqueous medium, requiring a complex co-solvent approach to obtain the nanocylinders: the polymer was first dissolved at 100 g/L in pure DMSO, a strong hydrogen bond competitor, followed by slow addition of water which triggered self-assembly into nanocylinders. These supramolecular structures could undergo *trans* → *cis* isomerization to a 25/75 ratio upon exposure to UV-light (365 nm); which led to their disruption into much smaller and mostly spherical particles. The disruption was however irreversible upon *cis* → *trans* back photo-isomerization at 450 nm; which we attributed to the kinetically frozen nature of the assemblies, likely induced by strong hydrophobic effects. These results are in agreement with work reported by Feringa et al., who showed that a stilbene-bisurea with oligo-PEO arms self-assembled in both water and toluene, with a Gibbs free energy two times higher in water, due to the hydrophobic effect; but for which isomerization was possible in toluene (to 33% *cis*)[16] but blocked in water at r.t., probably because of the hydrophobic effect contribution hampering reorganization in water.[17] Additionally, in the field of amphiphilic block copolymers, it was reported that very strong hydrophobic effects can prevent supramolecular structures from reaching thermodynamic equilibrium and to be reversibly stimuli-responsive.[22]

In chloroform and toluene, Azo-(U-PEO)$_2$ spontaneously formed SPBs upon direct dissolution. The azobenzene units of Azo-(U-PEO)$_2$ were able to photo-isomerize from *trans* to *cis* and from *cis* back to *trans*, when exposed to UV (365 nm) and blue light (450 nm), respectively. In both cases, photo-isomerization at 365 nm triggered disassembly, but irradiation at 450 nm reversibly conducted to the reformation of the nanocylinders. In toluene,

the disassembly was only partial, which we attribute to the fact that even after UV irradiation, some *trans* isomer is left (~25-30%, see **Figure S5**), possibly due to strong H-bonding somewhat hindering photo-isomerization and/or to the shift of absorption maximum of the *trans* isomer modifying the quantum yield of photo-isomerization. According to kinetic experiments performed by SAXS, the rate-limiting step for disassembly seems to be the *trans* → *cis* isomerization, implying a rather fast supramolecular organization of the *trans*-Azo-(U-PEO)$_2$ units into nanocylinders. The SPBs could be quantitatively recovered with blue light irradiation, since all of the azobenzenes photo-isomerized back to their *trans* configuration. In chloroform, on the other hand, near quantitative disruption of SPBs was achieved, which we attribute to the fact that chloroform is slightly more H-bond competing than toluene, thus weakening the assemblies and allowing an almost full *trans* → *cis* isomerization. Re-assembly was also achieved upon blue light irradiation, albeit to a lesser extent. Indeed, only 70% of the initial level of scattering was recovered, consistent with the fact that only 70% of *trans*-azobenzene was recovered upon blue light irradiation. All these results suggest that the supramolecular nanocylinders formed in toluene or chloroform by Azo-(U-PEO)$_2$ are under thermodynamic equilibrium, unlike what was observed in aqueous medium. This could be explained by the fact that the solvophobic effects were likely much weaker in these solvents, compared to water, and the assembly was mainly driven by H-bonding (**Scheme 2**).

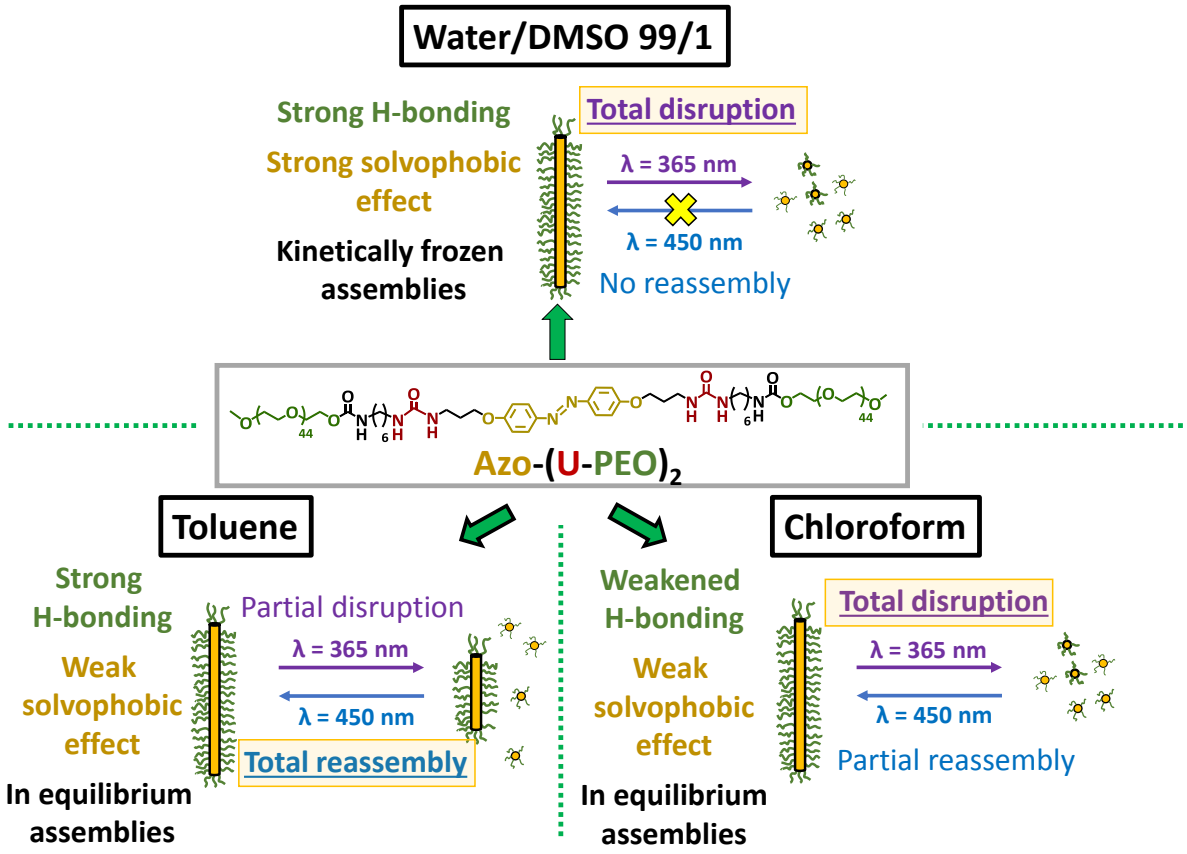

Scheme 2. Schematic representation of the different modes of self-assembly of Azo-(U-PEO)$_2$ in the three studied solvents.

Conclusions

Azo-(U-PEO)$_2$ is an azobenzene-bisurea self-assembling core decorated with PEO arms providing solubility in water, chloroform, and toluene. This molecule was previously shown to self-assemble into long supramolecular nanocylinders in aqueous medium, which could be disrupted into small particles upon *trans-cis* photo-isomerization.[11] However, the self-assembled structures are frozen in aqueous medium, probably due to strong hydrophobic effects, requiring a complex assembly procedure to form the nanocylinders and causing the photo-induced disruption of the nanocylinders to be irreversible.

In this work, we showed that the formation of long supramolecular nanocylinders is also possible in chloroform and toluene and that *trans* → *cis* photo-isomerization leads to a

reversible disassembly of the nanocylinders in these solvents. The amount of disrupted nanocylinders at photo-stationary state upon *trans* → *cis* photo-isomerization was in good agreement with the percentage of *trans*-Azo-(U-PEO)$_2$ transformed into *cis*-Azo-(U-PEO)$_2$. Moreover, the kinetics of disassembly in toluene-d$_8$ were of the same order of magnitude as the rate of *trans* → *cis* photo-isomerization, suggesting that the latter is the rate-limiting step in the photo-responsive disassembly.

This work highlights the role of the solvent, probably by changing the strength of solvophobic interactions, in controlling the kinetics of assembly and the stimuli-responsive nature of supramolecular self-assemblies. It moreover presents the first example of reversible light-triggered disassembly of SPBs to the best of our knowledge, opening the door for potential applications in various fields.

ACKNOWLEDGMENT

Le Mans Université is acknowledged for funding LH's PhD work. The authors thank Sandra Kalem for fruitful discussions. Sullivan Bricaud and plateforme "RMN" are thanked for help with NMR measurements. SANS beam time allocation from ILL is acknowledged (10.5291/ILL-DATA.9-11-2108). SAXS beam time allocation from ESRF is acknowledged (proposal number A02-1-916 on D2AM). Frederick Niepceron and Plateforme "Microscopie" at IMMM are thanked for attempts at imaging the nanocylinders by cryoTEM in toluene. This work benefited from the use of the SasView application, originally developed under NSF award DMR-0520547. SasView contains code developed with funding from the European Union's Horizon 2020 research and innovation programm under the SINE2020 project, grant agreement No 654000.

REFERENCES

(1) Hartlieb, M.; Mansfield, E. D. H.; Perrier, S. A Guide to Supramolecular Polymerizations. *Polym Chem* **2020**, *11* (6), 1083–1110. https://doi.org/10.1039/c9py01342c.

(2) Gruschwitz, F. V.; Klein, T.; Catrouillet, S.; Brendel, J. C. Supramolecular Polymer Bottlebrushes. *Chemical Communications* **2020**, *56* (38), 5079–5110. https://doi.org/10.1039/d0cc01202e.

(3) Palmer, L. C.; Stupp, S. I. Molecular Self-Assembly into One-Dimensional Nanostructures. *Acc Chem Res* **2008**, *41* (12), 1674–1684. https://doi.org/10.1021/ar8000926.

(4) Song, Q.; Goia, S.; Yang, J.; Hall, S. C. L.; Staniforth, M.; Stavros, V. G.; Perrier, S. Efficient Artificial Light-Harvesting System Based on Supramolecular Peptide Nanotubes in Water. *J Am Chem Soc* **2021**, *143* (1), 382–389. https://doi.org/10.1021/jacs.0c11060.

(5) Danial, M.; My-Nhi Tran, C.; Young, P. G.; Perrier, S.; Jolliffe, K. A. Janus Cyclic Peptide-Polymer Nanotubes. *Nat Commun* **2013**, *4*. https://doi.org/10.1038/ncomms3780.

(6) Han, S.; Pensec, S.; Yilmaz, D.; Lorthioir, C.; Jestin, J.; Guigner, J. M.; Niepceron, F.; Rieger, J.; Stoffelbach, F.; Nicol, E.; Colombani, O.; Bouteiller, L. Straightforward Preparation of Supramolecular Janus Nanorods by Hydrogen Bonding of End-Functionalized Polymers. *Nat Commun* **2020**, *11* (1), 2–7. https://doi.org/10.1038/s41467-020-18587-2.

(7) Nicolas, C.; Ghanem, T.; Canevet, D.; Sallé, M.; Nicol, E.; Gautier, C.; Levillain, E.; Niepceron, F.; Colombani, O. Oxidation-Sensitive Supramolecular Polymer Nanocylinders. *Macromolecules* **2022**, *55* (14), 6167–6175. https://doi.org/10.1021/acs.macromol.2c00879.

(8) Song, Q.; Yang, J.; Rho, J. Y.; Perrier, S. Supramolecular Switching of the Self-Assembly of Cyclic Peptide-Polymer Conjugates: Via Host-Guest Chemistry. *Chemical Communications* **2019**, *55* (36), 5291–5294. https://doi.org/10.1039/c9cc01914f.

(9) Otter, R.; Klinker, K.; Spitzer, D.; Schinnerer, M.; Barz, M.; Besenius, P. Folding Induced Supramolecular Assembly into PH-Responsive Nanorods with a Protein Repellent Shell. *Chemical Communications* **2018**, *54* (4), 401–404. https://doi.org/10.1039/c7cc08127h.

(10) Otter, R.; Berac, C. M.; Seiffert, S.; Besenius, P. Tuning the Life-Time of Supramolecular Hydrogels Using ROS-Responsive Telechelic Peptide-Polymer Conjugates. *Eur Polym J* **2019**, *110* (October 2018), 90–96. https://doi.org/10.1016/j.eurpolymj.2018.11.019.

(11) Harvey, L.; Guigner, J. M.; Bouteiller, L.; Nicol, E.; Colombani, O. Photo-Responsive Disassembly of Supramolecular Polymer Bottlebrushes in Water. **2023**, *14*, 4970-4978. https://doi.org/10.1039/D3PY00963G.

(12) Fatás, P.; Bachl, J.; Oehm, S.; Jiménez, A. I.; Cativiela, C.; Díaz Díaz, D. Multistimuli-Responsive Supramolecular Organogels Formed by Low-Molecular-Weight Peptides Bearing Side-Chain Azobenzene Moieties. *Chemistry - A European Journal* **2013**, *19* (27), 8861–8874. https://doi.org/10.1002/chem.201300796.

(13) Velema, W. A.; Stuart, M. C. A.; Szymanski, W.; Feringa, B. L. Light-Triggered Self-Assembly of a Dichromonyl Compound in Water. *Chemical Communications* **2013**, *49* (44), 5001–5003. https://doi.org/10.1039/c3cc41018h.

(14) Endo, M.; Fukui, T.; Jung, S. H.; Yagai, S.; Takeuchi, M.; Sugiyasu, K. Photoregulated Living Supramolecular Polymerization Established by Combining Energy Landscapes of Photoisomerization and Nucleation-Elongation Processes. *J Am Chem Soc* **2016**, *138* (43), 14347–14353. https://doi.org/10.1021/jacs.6b08145.

(15) Xu, J. F.; Chen, Y. Z.; Wu, D.; Wu, L. Z.; Tung, C. H.; Yang, Q. Z. Photoresponsive Hydrogen-Bonded Supramolecular Polymers Based on a Stiff Stilbene Unit. *Angewandte Chemie - International Edition* **2013**, *52* (37), 9738–9742. https://doi.org/10.1002/anie.201303496.

(16) Xu, F.; Pfeifer, L.; Crespi, S.; Leung, F. K. C.; Stuart, M. C. A.; Wezenberg, S. J.; Feringa, B. L. From Photoinduced Supramolecular Polymerization to Responsive Organogels. *J Am Chem Soc* **2021**, *143* (15), 5990–5997. https://doi.org/10.1021/jacs.1c01802.

(17) Xu, F.; Crespi, S.; Pfeifer, L.; Stuart, M. C. A.; Feringa, B. L. Mechanistic Insight into Supramolecular Polymerization in Water Tunable by Molecular Geometry. *CCS Chemistry* **2022**, *4* (7), 2212–2220. https://doi.org/10.31635/ccschem.022.202201821.

(18) Fuentes, E.; Gerth, M.; Berrocal, J. A.; Matera, C.; Gorostiza, P.; Voets, I. K.; Pujals, S.; Albertazzi, L. An Azobenzene-Based Single-Component Supramolecular Polymer Responsive to Multiple Stimuli in Water. *J Am Chem Soc* **2020**, *142* (22), 10069–10078. https://doi.org/10.1021/jacs.0c02067.

(19) Catrouillet, S.; Fonteneau, C.; Bouteiller, L.; Delorme, N.; Nicol, E.; Nicolai, T.; Pensec, S.; Colombani, O. Competition between Steric Hindrance and Hydrogen Bonding in the Formation of Supramolecular Bottle Brush Polymers. *Macromolecules* **2013**, *46* (19), 7911–7919. https://doi.org/10.1021/ma401167n.

(20) Han, S.; Mellot, G.; Pensec, S.; Rieger, J.; Stoffelbach, F.; Nicol, E.; Colombani, O.; Jestin, J.; Bouteiller, L. Crucial Role of the Spacer in Tuning the Length of Self-Assembled Nanorods. *Macromolecules* **2020**, *53* (1), 427–433. https://doi.org/10.1021/acs.macromol.9b01928.

(21) Yang, J.; Song, J. I.; Song, Q.; Rho, J. Y.; Mansfield, E. D. H.; Hall, S. C. L.; Sambrook, M.; Huang, F.; Perrier, S. Hierarchical Self-Assembled Photo-Responsive Tubisomes from a Cyclic Peptide-Bridged Amphiphilic Block Copolymer. *Angewandte Chemie - International Edition* **2020**, *59* (23), 8860–8863. https://doi.org/10.1002/anie.201916111.

(22) Nicolai, T.; Colombani, O.; Chassenieux, C. Dynamic Polymeric Micelles versus Frozen Nanoparticles Formed by Block Copolymers. *Soft Matter* **2010**, *6* (14), 3111–3118. https://doi.org/10.1039/b925666k.
(23) Crippa, M.; Perego, C.; de Marco, A. L.; Pavan, G. M. Molecular Communications in Complex Systems of Dynamic Supramolecular Polymers. *Nat Commun* **2022**, *13* (1), 1–12. https://doi.org/10.1038/s41467-022-29804-5.
(24) Skov Pedersen, J. *Form Factors of Block Copolymer Micelles with Spherical, Ellipsoidal and Cylindrical Cores*; 2000; Vol. 33.
(25) Choisnet, T.; Canevet, D.; Sallé, M.; Nicol, E.; Niepceron, F.; Jestin, J.; Colombani, O. Robust Supramolecular Nanocylinders of Naphthalene Diimide in Water. *Chemical Communications* **2019**, *55* (64), 9519–9522. https://doi.org/10.1039/c9cc04723a.

Graphical Abstract.